Original Article

DOI: 10.7860/JCDR/2026/89802.24174

Dentistry Section

# Bioactive Bilayered Chitosan-zinc Oxide/Polycaprolactone Scaffold with Controlled Barrier Function for Guided Bone Regeneration in Implant-related Diseases: An In-vitro Evaluation

SUPRAJA GOVINDARAJAN[1], ARVINA RAJASEKAR[2]



## ABSTRACT

**Introduction:** Peri-implant infectious diseases remain a significant challenge affecting implant success, human health, and oral well-being. Effective regeneration around dental implants requires restoration of peri-implant bone while limiting undesirable soft-tissue infiltration. Conventional single-layered barrier membranes provide mechanical occlusion but lack bioactivity to promote osteogenesis. Therefore, multifunctional scaffolds with regenerative potential and effective barrier function are needed to improve implant therapy and enhance regenerative outcomes in implant-related diseases.

**Aim:** To design, characterise, and assess the in-vitro regenerative potential of a bilayered Chitosan–Zinc Oxide/Polycaprolactone (CS–ZnO/PCL) scaffold integrating bioactivity with barrier function for implant-related disease regeneration.

**Materials and Methods:** The present in-vitro study was conducted in Saveetha Dental College and Hospitals, Chennai, Tamil Nadu, India, from September 2024 to January 2025. A bilayer scaffold was fabricated by combining a solvent-cast PCL layer with a porous CS-ZnO top layer. Morphology was analysed by Field Emission Scanning Electron Microscopy (FESEM). Functional group integration was confirmed via Fourier Transform Infrared (FTIR) spectroscopy. Surface wettability was measured by contact angle analysis. Haemocompatibility was assessed through an ASTM F756-compliant haemolysis assay. In-vitro fibroblast migration across the bilayer scaffold was evaluated over 14 days.

**Results:** The FESEM revealed a porous, interconnected CS-ZnO top layer suitable for tissue infiltration and a smooth, dense PCL base layer providing effective barrier characteristics. FTIR confirmed the incorporation of CS, ZnO, and PCL, with O-H stretching shifts indicative of hydrogen bonding. The scaffold exhibited enhanced hydrophilicity and haemolysis values <5%, meeting biocompatibility standards. Migration assays showed restricted fibroblast migration at day 7 and minimal penetration by day 14, indicating controlled cellular infiltration across the bilayer structure.

**Conclusion:** The CS-ZnO/PCL bilayer scaffold provides bioactivity with controlled barrier function, representing a promising material for guided bone regeneration and peri-implant tissue healing. This approach may improve implant outcomes, reduce the risk of peri-implant disease, and enhance patient well-being. The bilayered scaffold exhibited favourable physicochemical characteristics, indicating its potential as a candidate for implant-related bone regeneration.

**Keywords:** Disease, Nanoparticles, Peri-implant disease, Polymers, Scaffold

## INTRODUCTION

Dental implants have become a predictable and widely used treatment modality for the rehabilitation of missing teeth, significantly improving oral function, aesthetics, and patient well-being [1]. However, the long-term success of implant therapy is frequently challenged by implant-related diseases, particularly peri-implant mucositis and peri-implantitis, which are characterised by inflammatory destruction of peri-implant tissues and progressive bone loss [2]. These conditions arise from a complex interplay between microbial biofilms, host immune-inflammatory responses, implant surface characteristics, prosthetic design, occlusal overload, surgical trauma, residual cement, inadequate oral hygiene, systemic risk factors, and local anatomical factors [3-5].

To reduce the incidence of implant-related disease and enhance osseointegration, extensive research has focused on modifying implant surfaces and developing bioactive coatings [6,7]. Micro- and nano-topographical modifications, surface functionalisation, and incorporation of antimicrobial or osteogenic agents have been explored to improve bone–implant contact and limit bacterial colonisation [8,9]. Despite these advances, implant-related diseases continue to occur, often leading to peri-implant bone defects that compromise implant stability and function.

Consequently, regenerative strategies aimed at reconstructing lost peri-implant bone have gained increasing importance. Successful regeneration requires a coordinated interaction of cells, signalling molecules, and scaffolds that provide both structural support and biological cues [10]. A major limitation in implant-related regeneration is undesirable soft-tissue infiltration into the defect site, which may hinder osteogenic cell repopulation and impede bone formation. Therefore, biomaterials with combined bioactivity and effective barrier function are essential for implant-related disease regeneration [11].

Polycaprolactone (PCL), a synthetic biodegradable polymer, offers favourable mechanical strength and structural stability, making it suitable for space maintenance and barrier applications. However, its hydrophobic nature limits cellular interaction and bioactivity [12]. Chitosan (CS), a naturally derived polysaccharide, exhibits excellent biocompatibility, biodegradability, and bioactive properties that support osteogenic cell migration and extracellular matrix formation [13]. Incorporation of ZnO further enhances osteogenic potential

and provides antimicrobial activity, creating a microenvironment conducive to healing and reduced infection risk [14].

Previous studies have investigated the use of PCL-based membranes for guided bone regeneration owing to their favourable mechanical properties and ability to function as physical barriers [15,16]. Similarly, CS-based scaffolds have been extensively explored because of their biocompatibility, biodegradability, and ability to support cellular attachment and tissue regeneration [17]. However, most currently available regenerative membranes are either primarily passive barriers lacking biological activity or bioactive scaffolds with limited capability to effectively prevent undesirable soft-tissue infiltration [18]. Furthermore, there is limited evidence regarding bilayered scaffold systems that simultaneously integrate a dense barrier layer and a bioactive porous layer for periodontal and peri-implant regeneration [19,20]. Therefore, there is a need to develop multifunctional biomaterials capable of providing both guided tissue exclusion and active regenerative support. The novelty of the present study lies in the fabrication of a bilayered CS–ZnO/PCL scaffold that combines the barrier function of a dense PCL layer with the bioactivity of a porous CS–ZnO layer in a single construct.

Based on these considerations, the present study aimed to design, characterise, and evaluate the in-vitro regenerative potential of a CS–ZnO/PCL scaffold with integrated bioactivity and barrier function for implant-related disease regeneration. The PCL layer was intended to restrict undesirable soft-tissue infiltration, while the porous CS–ZnO layer is designed to provide a microenvironment potentially favourable for angiogenesis, osteogenesis and antimicrobial activity.

## MATERIALS AND METHODS

The present in-vitro study was conducted in Saveetha Dental College and Hospitals, Chennai, Tamil Nadu, India, from September 2024 to January 2025. The ethical approval for this study was obtained from the institute's Scientific Review Board (SRB/SDC/PERIO-2301/24/328).

**Inclusion and Exclusion criteria:** As this was an in-vitro study, conventional participant-based inclusion and exclusion criteria were not applicable. Only successfully fabricated bilayered CS–ZnO/PCL scaffolds exhibiting intact structural integrity, adequate interlayer adhesion, and absence of visible defects were included for characterisation and biological evaluation. Human gingival fibroblast cultures demonstrating normal morphology and viability were included for the cell migration assay, and fresh peripheral blood obtained from a healthy donor was used for haemocompatibility testing. Scaffold specimens showing fabrication defects, contamination, delamination, or structural damage were excluded from the study. Additionally, contaminated or non viable cell cultures and blood samples exhibiting pre-existing haemolysis or other abnormalities were excluded from experimental analyses.

### Study Procedure

Synthesis of the bi-layered CS-ZNO/PCL scaffold-

**Synthesis of Zinc Oxide nanoparticles (ZnO NPs):** Zinc oxide nanoparticles were synthesised via a wet chemical precipitation method. Briefly, 100 mL of 0.2 M Sodium Hydroxide (NaOH) solution was added dropwise to 100 mL of 0.1 M Zinc Nitrate hexahydrate $\{Zn(NO_3)_2 \cdot 6H_2O\}$ solution under continuous magnetic stirring [Table/Fig-1]. The reaction was maintained at ambient temperature for four hours to ensure complete precipitation. The resulting white precipitate was collected by vacuum filtration, thoroughly washed with deionised water to remove residual ions, and dried at 100°C. The dried powder was subsequently calcined at 400°C for two hours to obtain crystalline ZnO nanoparticles (ZnO NccPs) [21].

**Preparation of Chitosan (CS) Scaffold incorporating ZnO NPs:** The CS powder (0.5 g) was dissolved in 100 mL of 2% (v/v) acetic acid under constant stirring until a homogeneous solution was achieved. Synthesised ZnO NPs were incorporated into the CS solution at a concentration of 1 wt%, followed by thorough mixing to ensure uniform dispersion. The resulting CS-ZnO mixture was cast into sterile petri-dishes and frozen at -80°C. The frozen samples were lyophilised at -110°C to produce a porous CS-ZnO scaffold through ice crystal sublimation [Table/Fig-2] [22].

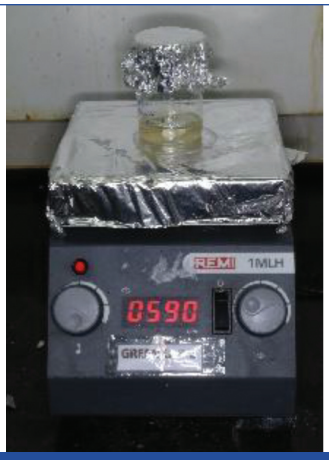


**[Table/Fig-1]:** Sodium hydroxide (NaOH) and Zinc Nitrate hexahydrate {Zn(NO3)2·6H2O} solution under continuous magnetic stirring.

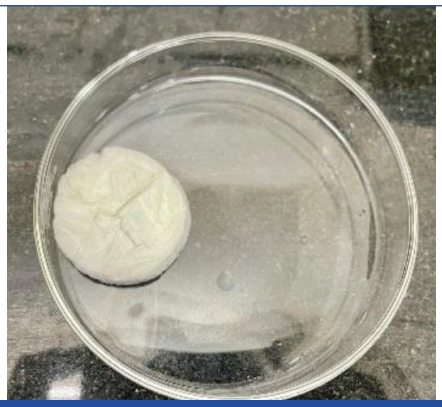

**[Table/Fig-2]:** Chitosan-Zinc Oxide mixture cast into sterile petri-dishes to obtain a porous CS-ZnO scaffold.

**Fabrication of Polycaprolactone (PCL) Layer:** The PCL granules (1g) were dissolved in 10 mL of chloroform with gentle stirring. The solution was cast into glass petri-dishes and left undisturbed at room temperature to allow complete solvent evaporation, resulting in a uniform PCL film [Table/Fig-3] [23].

**[Table/Fig-3]:** Uniform PCL film after complete solvent evaporation.

**Assembly of the Bi-layered scaffold:** A novel bilayered fabrication method was developed in the present study, wherein a pre-fabricated CS-ZnO scaffold was placed onto a partially dried PCL film to achieve interlayer adhesion through controlled solvent evaporation [Table/Fig-4].

**[Table/Fig-4]:** Bilayered scaffold obtained after complete chloroform evaporation.

### Characterisation Studies

**Morphological evaluation:** The surface morphology and microarchitecture of the PCL and CS-ZnO surfaces were examined using FESEM (ZEISS Gemini SEM 460). Before imaging, all specimens were sputter-coated with a thin gold layer (Edwards S150B, Crawley, UK) at 15 kV for 2.5 min to enhance conductivity. Imaging was performed at an accelerating voltage of 5 kV [24].

**Surface wettability assessment:** The hydrophilicity of scaffold surfaces was determined using a contact angle goniometer (Ossila, UK). A 5µL droplet of distilled water was carefully placed on the surface of each sample, and contact angles were recorded using video capture and analysed with Ossila software. Measurements were taken separately for PCL and CS-ZnO surfaces [25].

**Fourier Transform Infrared Spectroscopy (FTIR):** The FTIR was performed to identify functional groups and verify molecular composition (Bruker, Germany). Spectra were acquired for both CS-PCL and CS-ZnO/PCL scaffolds to confirm the incorporation of ZnO NPs and the characteristic peaks of each scaffold component [26].

**Haemocompatibility (haemolysis assay):** Human peripheral blood was collected from a healthy donor into heparinised tubes. Blood was centrifuged at 750 rpm for five min at 4°C to separate Red Blood Cells (RBCs) from plasma. The RBC pellet was washed three times with phosphate-buffered saline (PBS, pH 7.4). CS-ZnO/PCL scaffolds at concentrations of 5 mg/mL and 10 mg/mL were immersed in 2.5 mL of RBC suspension and incubated at 37°C for one hour. After incubation, samples were centrifuged, and the Optical Density (OD) of the supernatant was measured at 540 nm using a spectrophotometer [25]. Haemolysis percentage was calculated using:

Haemolysis (%) = {(OD sample - OD negative control)/(OD positive control - OD negative control)} × 100

The positive control consisted of RBCs suspended in distilled water, while RBCs incubated in PBS served as the negative control. All experiments were conducted in triplicate (n=3).

**Cell migration assay:** Cell migration was assessed using cell-crown inserts. Circular scaffold discs (25 mm diameter) were prepared and sterilised under UV light for two hours. Discs were positioned inside a 6-well culture plate to remain suspended without touching the well bottom. Human gingival fibroblast cells were cultured in Dulbecco's Modified Eagle Medium (DMEM) supplemented with 10% fetal bovine serum and 1% antibiotic solution. For the assay, 1 mL of cell-free DMEM was added to each well, and 1 mL of fibroblast suspension was seeded directly onto the PCL surface of the scaffold. Plates were incubated at 37°C in a humidified atmosphere containing 5% $CO_2$. Cell migration through the scaffold was evaluated at day 7 and day 14 using a light microscope (40× magnification) to assess controlled fibroblast infiltration across the bilayer structure [20].

## STATISTICAL ANALYSIS

Statistical analyses were performed using IBM Statistical Package for the Social Sciences (SPSS) Statistics 23.0. Quantitative data obtained from the haemolysis assay and surface wettability were expressed as mean±Standard Deviation (SD) based on three independent replicates (n=3). Descriptive statistical analysis was performed to summarise the data and evaluate the reproducibility of the results. An Independent t-test was performed to compare contact-angle measurements between scaffold layers. Qualitative observations from FESEM, FTIR, and cell migration analyses were interpreted descriptively.

## RESULTS

### FESEM Analysis

The FESEM images revealed distinct surface morphologies for each layer of the bilayer scaffold [Table/Fig-5]. The PCL layer exhibited a smooth, compact surface with minimal porosity, interspersed with linear, fibre-like ridges indicative of structural coherence and mechanical stability. In contrast, the CS-ZnO layer displayed a highly porous and interconnected network, with a rough, granular texture attributable to the incorporation of ZnO nanoparticles. These nanoparticles were uniformly distributed within the chitosan matrix, suggesting efficient dispersion and strong material compatibility.

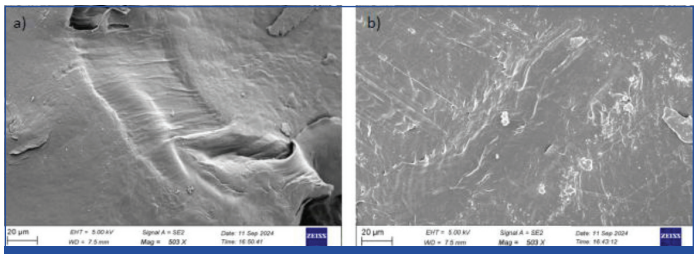


**[Table/Fig-5]:** FESEM images of the bi-layered scaffold: a) PCL layer showing a relatively smoother surface; and b) CS-ZnO layer showing a porous interconnected surface.

### Contact Angle Measurement

Surface wettability assessment demonstrated marked differences between the scaffold layers [Table/Fig-6]. The CS-ZnO surface exhibited higher hydrophilicity, reflected in its lower contact angle of 58.64±2.7, whereas the PCL surface displayed pronounced hydrophobicity with a contact angle of approximately 83.39±2.3 [Table/Fig-7], indicating reduced wettability. This wettability gradient across the bilayer may support differential cellular interaction, enabling the CS-ZnO layer to promote cell attachment and proliferation while the PCL layer serves as a structural barrier.

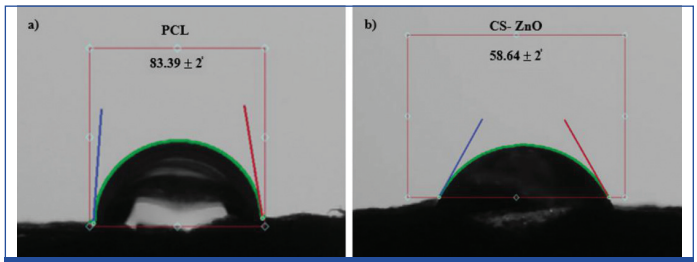


**[Table/Fig-6]:** Contact angle measurement of the: a) PCL has an obtuse angle signifying its hydrophobicity, b) CS-ZnO layer showing an acute angle indicative of its hydrophilicity.

| Scaffold | Mean±SD |
|---|---|
| PCL | 83.39±2.3 |
| CS-ZnO | 58.64±2.7 |

**[Table/Fig-7]:** Table displaying mean and Standard Deviation (SD) of the contact angle measurement for PCL layer and CS- ZnO layer.

FTIR Analysis FTIR spectroscopy confirmed the presence of characteristic functional groups corresponding to CS, PCL, and ZnO [Table/Fig-8]. The CS spectrum showed a broad band between

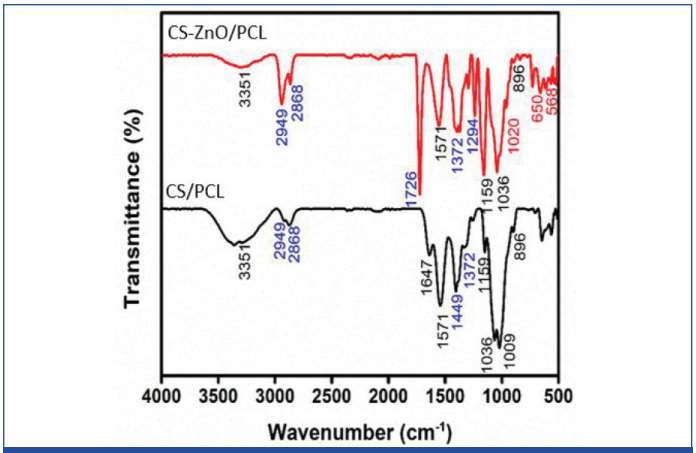


**[Table/Fig-8]:** FTIR spectra of the bi-layered scaffold with peaks indicating the presence of PCL, Chitosan, and Zinc oxide, and suggestive of the interactions between PCL and ZnO.

3000–3600 $cm^{-1}$ (O-H stretching), peaks at 1640-1655 $cm^{-1}$ (amide I), 1550–1650 $cm^{-1}$ (amide II), 1020-1150 $cm^{-1}$ (C–O stretching), and a band at 896 $cm^{-1}$ (CH bending). PCL exhibited peaks at 1726 $cm^{-1}$ (C=O stretching), 1294 $cm^{-1}$ (C-C and C-O stretching), 2949 and 2860 $cm^{-1}$ ($CH_2$ stretching), and 1449 and 1372 $cm^{-1}$ ($CH_2$ bending). ZnO showed characteristic peaks at 400–600 $cm^{-1}$ (Zn-O stretching), a band at 568 $cm^{-1}$ (hexagonal phase ZnO), and a peak near 1020 $cm^{-1}$ (Zn-O-Zn bonding). Notably, incorporation of ZnO into the CS matrix led to a reduction in the O-H stretching intensity, suggesting possible hydrogen bonding or coordination interactions between ZnO nanoparticles and CS chains.

### Haemolysis Assay

Haemolysis testing confirmed that both concentrations exhibited haemolysis percentages well below the American Society for Testing and Materials (ASTM) threshold of 5% for blood-contacting biomaterials [27], indicating excellent haemocompatibility [Table/Fig-9]. At 5 mg/mL, the haemolysis percentage was approximately 1.25±0.1%, while at 10 mg/mL it was 1.48±0.12%, confirming that scaffold concentration within the tested range does not adversely affect RBC integrity. These findings demonstrated that the CS-ZnO/PCL scaffold is safe for potential applications involving direct blood contact.

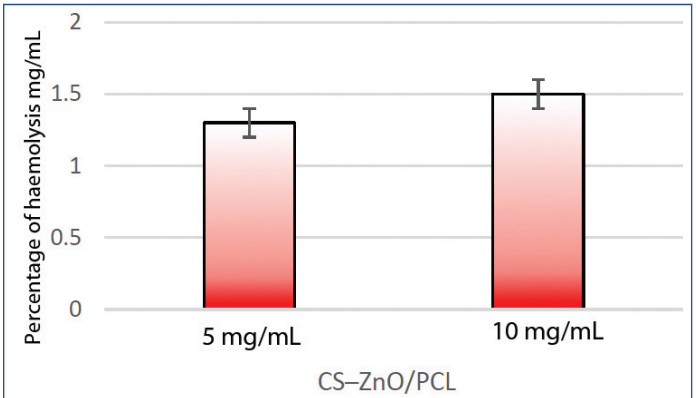


**[Table/Fig-9]:** Haemolysis graph of the scaffold confirming its high haemocompatibility with <5% haemolysis.

### Cell Migration Assay

The fibroblast migration assay [Table/Fig-10] demonstrated time-dependent cellular migration across the bilayer scaffold. On day 7, no fibroblasts were detected at the well bottom, indicating restricted early migration. By day 14, limited fibroblast presence was observed, suggesting controlled and gradual cell movement. This delayed migration behaviour reflects the bilayer architecture, where the dense PCL layer provides a temporary barrier, while the porous CS-ZnO layer supports guided fibroblast infiltration and tissue regeneration.

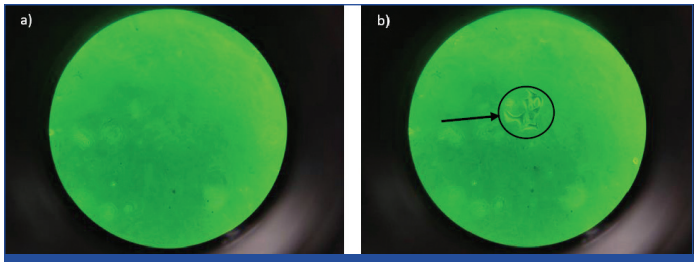


**[Table/Fig-10]:** Cell migration assay showing the bottom surface of the culture plate (a) Day 7 demonstrating no detectable fibroblast migration across the scaffold, (b) Day 14 showing limited fibroblast presence (arrow), indicating controlled cellular infiltration through the bilayer structure.

## DISCUSSION

Implant-related regenerative therapy aims to restore lost peri-implant bone while limiting undesirable soft-tissue infiltration into the defect area. Conventional single-layer barrier membranes used in guided bone regeneration primarily function as passive physical barriers; however, they are often biologically inert and lack the ability to actively promote osteogenesis. In clinical practice, bone grafts are frequently combined with membranes to enhance osteogenic activity and peri-implant tissue regeneration. Despite these approaches, early soft-tissue infiltration into peri-implant defects may compromise bone regeneration and reduce implant stability. These limitations highlight the need for multifunctional scaffolds that combine barrier properties with bioactive features capable of supporting peri-implant bone regeneration.

The bilayered scaffold developed in this study was engineered to address these dual requirements. The CS-ZnO top layer exhibited a porous, interconnected architecture, as confirmed by FESEM, which is favourable for cellular adhesion, nutrient diffusion, and vascular infiltration- factors critical for peri-implant bone regeneration. Wang X et al., demonstrated that porous interconnected scaffolds facilitate endothelial cell infiltration, migration, and proliferation, thereby promoting angiogenesis [28]. In contrast, the PCL base layer displayed a smoother and less porous morphology, making it suitable for limiting undesirable cellular infiltration. The influence of reduced porosity on limiting cell adhesion has been emphasized by Wang Z et al., who reported that scaffold morphology directly affects cellular attachment [29]. Comparable multilayered PCL-based membranes have also been shown to combine mechanical stability with effective barrier function [24], supporting guided bone regeneration around implants.

FTIR spectroscopy confirmed the integration of CS, PCL, and ZnO, each contributing distinct functionalities. ZnO incorporation into the CS matrix induced shifts in the O-H stretching region, suggesting hydrogen bonding or coordination interactions-mechanisms known to improve mechanical strength and hydrophilicity, thereby enhancing cell-material interactions. Han X et al., reported similar effects in cellulose-based scaffolds reinforced via hydrogen bonding [30]. ZnO nanoparticles further enhance scaffold performance through inherent antimicrobial properties and by promoting osteoblastic differentiation via reactive oxygen species generation and zinc ion release, essential cofactors in bone metabolism. Amin N et al., have described zinc's role in bone health through modulation of the RANK/RANKL/OPG pathway [31]. Furthermore, the enhanced hydrophilicity of the CS-ZnO surface observed in contact angle analysis is associated with improved fibroblast attachment and proliferation, as reported by Papenburg BJ et al., indicating its potential for peri-implant tissue healing [32].

Biological evaluation further supported the scaffold's potential for implant-related applications. The haemolysis assay demonstrated values below 5%, satisfying ASTM F756 standards and indicating excellent haemocompatibility. This property is particularly important for implant-related regenerative procedures, where materials come into immediate contact with blood and influence clot formation and early wound healing. The fibroblast migration assay provided

functional evidence of the scaffold's barrier behaviour. The bilayer structure restricted fibroblast migration during the initial seven days, and only limited cellular presence was observed by day 14. This controlled cellular infiltration suggests that the dense PCL layer acts as a temporary barrier, while the porous CS-ZnO layer supports gradual cell infiltration and tissue regeneration. Such controlled migration is desirable for maintaining a protected regenerative environment during early peri-implant healing. This controlled migration behaviour is comparable to previously reported PCL-based multilayer membranes [24], suggesting that the bilayer design may help maintain a favourable environment for early peri-implant bone regeneration.

Overall, the bilayered CS-ZnO/PCL scaffold demonstrated a synergistic combination of bioactivity and barrier function. The porous CS-ZnO layer provides a favourable microenvironment for peri-implant tissue regeneration, while the dense PCL layer restricts premature soft-tissue infiltration.

### Limitation(s)

The present study has certain limitations that should be acknowledged. Although the bilayered CS-ZnO/PCL scaffold exhibited promising physicochemical characteristics and biological performance, the findings are primarily derived from in-vitro evaluations. The cell migration assay was qualitative and lacked a quantitative assessment, which may limit the accuracy of interpretation. In addition, key parameters such as long-term degradation behaviour, mechanical stability under functional loading, and sustained bioactivity were not evaluated. The absence of in-vivo validation further restricts the direct extrapolation of these findings to clinical scenarios. Therefore, future investigations incorporating quantitative cellular analyses, detailed mechanical characterisation, antimicrobial evaluation, and well-designed in-vivo studies are essential to establish the clinical applicability of this scaffold in peri-implant tissue regeneration.

## CONCLUSION(S)

The bilayer scaffold composed of CS-ZnO/PCL demonstrated favourable physicochemical characteristics, excellent hemocompatibility, and controlled barrier function. The porous CS-ZnO layer supports cellular interaction and may promote osteogenic responses, while the dense PCL layer restricts early soft-tissue infiltration. These combined properties address limitations of conventional single-layer membranes and suggest that the bilayer scaffold holds promise for the regeneration of implant-related disease defects and guided bone regeneration applications.

## REFERENCES


[1] Alghamdi HS, Jansen JA. The development and future of dental implants. Dent Mater J. 2020;39(2):167-72.
[2] Klinge B, Klinge A, Bertl K, Stavropoulos A. Peri-implant diseases. Eur J Oral Sci. 2018;126:88-94.
[3] Yadalam PK, Sharma S, Natarajan PM, Ardila CM. Gradient boosting-based classification of interactome hub genes in periimplantitis with periodontitis–an integrated bioinformatic approach. Front Oral Health. 2024;5:1462845.
[4] Janagarathinam P, Rajasekar A. Oxidant and antioxidant status of peri-implant crevicular fluid in patients with sandblasted acid-etched and anodised dental implants: A prospective clinical study. J Osseointegration. 2025;17(3):140-47.
[5] Yadalam PK, Ardila CM. Deep neural networks based on Sp7 protein sequence prediction in peri-implant bone formation. Int J Dent. 2025;2025(1):7583275.
[6] Biju D, Arumugam P, Kannan S, Yadalam PK, Ronsivalle V, Cicciù M, et al. Development, characterization, and biocompatibility and corrosion analyses of a silver-decorated graphene oxide and chitosan surface coating for titanium dental implants: A preliminary report. Dent Med Probl. 2024;61(4):627-32.
[7] Kothari V, Rajaraman V, Ariga P, Sekaran S, Ganapathy DM. Antibacterial efficacy and antioxidant potential of hafnium-coated titanium implants: An in-vitro assessment. J Clin Diagn Res. 2025;19(8):ZC21-ZC25.
[8] Maiti S, Dhakshinya M, Nallaswamy D, Jessy P. Comparative analysis of surface characteristics and hardness of three dimensional printed PEEK vs PEKK-as implant biomaterial. J Osseointegration. 2024;16(1):16-22.
[9] Nahata B, Maiti S, Ganesh MK, Heboyan A, Sai L, Paulraj J. Sulfonated polyether ketone ketone (SPEKK) implant as an alternative to titanium implant-in-vivo study on Wistar Albino rat mandible. BMC Oral Health. 2025;25(1):557.
[10] Wang F, Cai X, Shen Y, Meng L. Cell-scaffold interactions in tissue engineering for oral and craniofacial reconstruction. Bioact Mater. 2022;23:16-44.
[11] Donos N, Akcali A, Padhye N, Sculean A, Calciolari E. Bone regeneration in implant dentistry: Which are the factors affecting the clinical outcome? Periodontol 2000. 2023;93(1):26-55.
[12] Malikmammadov E, Tanir TE, Kiziltay A, Hasirci V, Hasirci N. PCL and PCL-based materials in biomedical applications. J Biomater Sci Polym Ed. 2018;29(7-9):863-93.
[13] Ressler A. Chitosan-based biomaterials for bone tissue engineering applications: A short review. Polymers (Basel). 2022;14(16):3430.
[14] Wiesmann N, Mendler S, Buhr CR, Ritz U, Kämmerer PW, Brieger J. Zinc oxide nanoparticles exhibit favour able properties to promote tissue integration of biomaterials. Biomedicines. 2021;9(10):1462.
[15] Jin F, Zhou Z, Jiang D, Wang Y, Wang X, Zhang X. A novel PCL fiber membrane with a gradient structure for guided bone regeneration. RSC Adv. 2026;16(23):21066-78.
[16] Gedik B, Erdem MA. Electrospun PCL membranes for localized drug delivery and bone regeneration. BMC Biotechnol. 2025;25:31.
[17] Rahaman J, Reza A, Nasare D, Susanth J, Mukherjee D. Chitosan-based composite scaffolds for bone tissue engineering: Design strategies, mechanisms, and emerging roles in osteoimmunomodulation. Mater Today Commun. 2025;49:113948.
[18] Abtahi S, Chen X, Shahabi S, Nasiri N. Resorbable membranes for guided bone regeneration: Critical features, potentials, and limitations. ACS Mater Au. 2023;3(5):394-417.
[19] Lian M, Han Y, Sun B, Xu L, Wang X, Ni B, et al. A multifunctional electrowritten bi-layered scaffold for guided bone regeneration. Acta Biomater. 2020;118:83-99.
[20] Fu L, Wang Z, Dong S, Cai Y, Ni Y, Zhang T, et al. Bilayer Poly(Lactic-co-glycolic acid)/Nano-Hydroxyapatite membrane with barrier function and osteogenesis promotion for guided bone regeneration. Materials (Basel). 2017;10(3):257.
[21] Taka G, Das TD. Synthesis of ZnO nanoparticles through a simple wet chemical precipitation method. IOP Conf Ser Earth Environ Sci. 2022;1042:012017.
[22] Ullah S, Zainol I, Idrus RH. Incorporation of zinc oxide nanoparticles into chitosan-collagen 3D porous scaffolds: Effect on morphology, mechanical properties and cytocompatibility of 3D porous scaffolds. Int J Biol Macromol. 2017;104(Pt A):1020-29.
[23] Holešová S, Čech Barabaszová K, Hundáková M, Ščuková M, Hrabovská K, Joszko K, et al. Development of novel thin polycaprolactone (PCL)/clay nanocomposite films with antimicrobial activity promoted by the study of mechanical, thermal, and surface properties. Polymers (Basel). 2021;13(18):3193.
[24] Aldemir Dikici B, Dikici S, Reilly GC, MacNeil S, Claeyssens F. A novel bilayer polycaprolactone membrane for guided bone regeneration: Combining electrospinning and emulsion templating. Materials (Basel). 2019;12(16):2643.
[25] Velraj MS, Rajasekar A. Bio-functional azithromycin loaded polyvinyl alcohol and fucoidan hydrogel coating for titanium implants: An experimental in-vitro study. J Oral Biol Craniofac Res. 2025;15(5):1043-50.
[26] Pangesty A, Todo M. Improvement of mechanical strength of tissue engineering scaffold due to the temperature control of polymer blend solution. J Funct Biomater. 2021;12:47.
[27] Henkelman S, Blanton J, Oeveren W. Standardization of incubation conditions for hemolysis testing of biomaterials. Mater Sci Eng C. 2009;29:1650-54.
[28] Wang X, Lin M, Kang Y. Engineering porous β-tricalcium phosphate (β-TCP) scaffolds with multiple channels to promote cell migration, proliferation, and angiogenesis. ACS Appl Mater Interfaces. 2019;11(9):9223-32.
[29] Wang Z, Qing Q, Chen X, Liu CJ, Luo JC, Hu JL, et al. Effects of scaffold surface morphology on cell adhesion and survival rate in vitreous cryopreservation of tenocyte-scaffold constructs. Appl Surf Sci. 2016;388:223-27.
[30] Han X, Wu W, Wang J, Tian Z, Jiang S. Hydrogen-bonding-aided fabrication of wood derived cellulose scaffold/aramid nanofiber into high-performance bulk material. Materials (Basel). 2021;14(18):5444.
[31] Amin N, Clark CC, Taghizadeh M, Djafarnejad S. Zinc supplements and bone health: The role of the RANKL-RANK axis as a therapeutic target. J Trace Elem Med Biol. 2020;57:126417.
[32] Papenburg BJ, Rodrigues ED, Wessling M, Stamatialis D. Insights into the role of material surface topography and wettability on cell-material interactions. Soft Matter. 2010;6(18):4377-88.

**PARTICULARS OF CONTRIBUTORS:**
1. Postgraduate Student, Department of Periodontics, Saveetha Dental College and Hospital, Saveetha Institute of Medical and Technical Sciences (SIMATS), Chennai, Tamil Nadu, India.
2. Associate Professor, Department of Periodontics, Saveetha Dental College and Hospital, Saveetha Institute of Medical and Technical Sciences (SIMATS), Chennai, Tamil Nadu, India.

**NAME, ADDRESS, E-MAIL ID OF THE CORRESPONDING AUTHOR:**
Arvina Rajasekar,
Associate Professor, Department of Periodontics, Saveetha Dental College and Hospital, Saveetha Institute of Medical and Technical Sciences (SIMATS), NH48, Chennai, Tamil Nadu, India.
E-mail: arvinar.sdc@saveetha.com

**PLAGIARISM CHECKING METHODS:** [Jain H et al.]
- Plagiarism X-checker: Apr 27, 2026
- Manual Googling: Jun 15, 2026
- iThenticate Software: Jun 17, 2026 (1%)

**ETYMOLOGY:** Author Origin

**EMENDATIONS:** 6

**AUTHOR DECLARATION:**
- Financial or Other Competing Interests: None
- Was Ethics Committee Approval obtained for this study? Yes
- Was informed consent obtained from the subjects involved in the study? NA
- For any images presented appropriate consent has been obtained from the subjects. NA

Date of Submission: **Apr 15, 2026**
Date of Peer Review: **May 23, 2026**
Date of Acceptance: **Jun 19, 2026**
Date of Publishing: **Aug 01, 2026**